Correlating Calmodulin Landscapes with Chemical Catalysis in Neuronal Nitric Oxide Synthase using Time-Resolved FRET and a 5-Deazaflavin Thermodynamic Trap

Tobias M. Hedison, Nicole G. H. Leferink, Sam Hay, and Nigel S. Scrutton*

Manchester Synthetic Biology Research Centre for Fine and Speciality Chemicals (SYNBIOCHEM), Manchester Institute of Biotechnology, The University of Manchester, Manchester M1 7DN, United Kingdom

S *Supporting Information*

ABSTRACT: A major challenge in enzymology is the need to correlate the dynamic properties of enzymes with, and understand the impact on, their catalytic cycles. This is especially the case with large, multicenter enzymes such as the nitric oxide synthases (NOSs), where the importance of dynamics has been inferred from a variety of structural, single-molecule, and ensemble spectroscopic approaches but where motions have not been correlated experimentally with mechanistic steps in the reaction cycle. Here we take such an approach. Using time-resolved spectroscopy employing absorbance and Förster resonance energy transfer (FRET) and exploiting the properties of a flavin analogue (5-deazaflavin mononucleotide (5-dFMN)) and isotopically labeled nicotinamide coenzymes, we correlate the timing of CaM structural changes when bound to neuronal nitric oxide synthase (nNOS) with the nNOS catalytic cycle. We show that remodeling of CaM occurs early in the electron transfer sequence (FAD reduction), not at later points in the reaction cycle (e.g., FMN reduction). Conformational changes are tightly correlated with FAD reduction kinetics and reflect a transient "opening" and then "closure" of the bound CaM molecule. We infer that displacement of the C-terminal tail on binding NADPH and subsequent FAD reduction are the likely triggers of conformational change. By combining the use of cofactor/coenzyme analogues and time-resolved FRET/absorbance spectrophotometry, we show how the reaction cycles of complex enzymes can be simplified, enabling a detailed study of the relationship between protein dynamics and reaction cycle chemistry—an approach that can also be used with other complex multicenter enzymes.

KEYWORDS: *nitric oxide synthase, calmodulin, Förster resonance energy transfer, protein dynamics, flavoenzyme, flavin analogue*
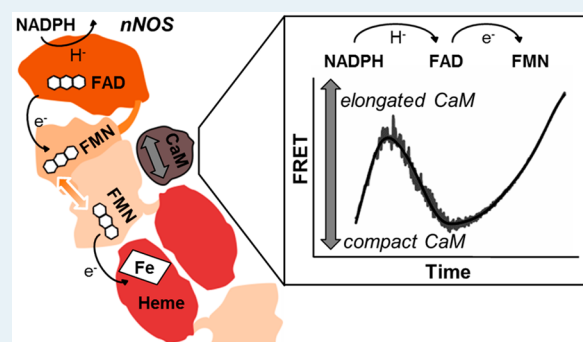
INTRODUCTION

Underpinning the function of all enzymes is the concept of protein conformational landscapes, knowledge of which is essential also in the rational design of synthetic proteins[1,2] and in the drug discovery process.[3,4] Many structure determination techniques (e.g., X-ray crystallography) have produced "frozen" snapshots of proteins that provide mechanistic insights into function. The drawback is that these snapshots typically represent only the lowest energy state of the many substates found within the conformational landscape of a dynamic protein. It is widely perceived that the interchange between individual conformers contributes, in part, toward the ability of an enzyme to enhance the rate of catalysis[5−9] and gate chemical steps,[10−12] as well as impart specificity for substrates.[4,13,14] The interchange between different conformations occurs over several angstroms, on time scales that span picoseconds to seconds. Many biophysical techniques can be used to probe the modulation of energy landscapes: for example, following the binding of ligands/inhibitors/partner proteins,[14−18] or changes in temperature, ionic strength, and pressure.[12,19−21] However,

fewer studies have focused on the detection of transient conformations that appear during enzyme catalysis. Likewise, little information is available on the mechanistic trigger(s) for these conformational transitions (e.g., substrate binding/product release and/or chemical steps). Understanding the nature and impact of short-lived high-energy conformational states on enzyme function is currently a topic of major interest.

A protein whose dynamic properties have been studied extensively is calmodulin (CaM).[22−29] CaM is a small, ubiquitous protein involved in the regulation of many biological processes in eukaryotes.[30] By binding Ca^{2+}, CaM undergoes major conformational change, shifting from a "closed" form to an extended "dumbbell" shape by the separation of two globular and structurally related calcium-binding domains. Once CaM adopts this "open" conformation, numerous hydrophobic residues on its surface are exposed, increasing

the affinity of CaM for a variety of partner proteins.[23] One such partner is the flavohemoprotein neuronal nitric oxide synthase (nNOS), for which CaM binding is essential for function.[31,32] nNOS is one of three tissue-specific isoforms of nitric oxide synthase (NOS), all of which are homodimers and produce L-citrulline and the signaling molecule nitric oxide (NO) from NADPH, dioxygen, and L-arginine.[31] Despite the lack of atomic level structural data for full-length nNOS holo-enzyme, a structural and mechanistic model (Figure 1) has emerged from a wealth of spectroscopic data[20,32−51] and determined structures of component NOS domains.[52−57]
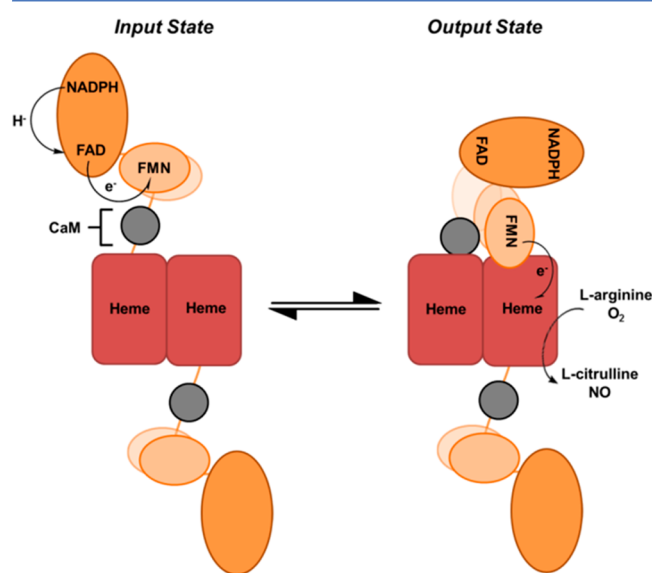

Figure 1. Structural organization and electron flow through nitric oxide synthase (NOS). The FAD domain is shown in bright orange, the FMN domain in light orange, the heme domain in red, and the partner protein calmodulin (CaM) in in gray. Ligand (NADPH and CaM) binding is implicated in shifting the conformational equilibrium of nNOS and thus regulating electron transfer during the catalytic cycle. Dimerization of nNOS occurs at an interface between the heme domains.

Each nNOS monomer comprises a reductase and an oxygenase domain separated by a CaM binding region. The reductase domain is structurally similar to cytochrome P450 reductase (CPR)[56,58] and encompasses FAD- and FMN-binding domains separated by a connecting domain and a flexible linker. Individual nNOS monomers dimerize at the interface of the oxygenase domains, which contain a regulatory PDZ domain and a heme domain. The heme domains also contain tightly bound heme and tetrahydrobiopterin (H$_4$B) cofactors. On binding to NOS, Ca^{2+}-bound CaM undergoes a conformational transition from an elongated "open" structure to a compact, spherical-shaped conformation.[57,59] These structural transitions are accompanied by changes in nNOS as the protein occupies energetically more favored conformations.[41,45]

Large-scale domain motion (>10 Å) influenced by CaM binding is believed to regulate electron transfer in NOS enzymes (Figure 1).[18,20,55] Catalysis is initiated by the binding of the reducing coenzyme NADPH to the FAD-binding domain and hydride transfer to the N5 position of the FAD isoalloxazine ring.[33] Interflavin electron transfer from the FAD cofactor to FMN then follows.[33,60] On reduction of the FMN,

electrons are transferred to the heme domain in the partner monomer of the enzyme dimer[47−49] where NO is produced. FMN to heme electron transfer requires the presence of CaM, which is essential also for NO production.[32,47,61] On the basis of spectroscopic and structural data, shuttling of the FMN domain between the FAD and heme domains is thought to be a feature of the natural catalytic cycle (Figure 1).[18,55]

The two flavin cofactors are juxtaposed when electrons are transferred from the FAD to FMN domains, allowing for efficient interflavin electron transfer in the "input" state (Figure 1).[18,55,56] Given the relatively large distance between the FMN and heme cofactors in the "input" state, electron transfer between the reductase and oxygenase domains does not occur unless there is movement of the FMN domain toward the oxygenase domain (the so-called "output" state). These shifts from "input" to "output" states are regulated by CaM binding[61] and have been studied using a variety of spectroscopic techniques, including fluorescence,[44,62−64] single-molecule fluorescence,[45] electron paramagnetic resonance,[20,42,43] cryo-electron microscopy,[39,40,65] and temperature jump spectroscopy.[35] However, to the best of our knowledge, there are no reported studies that have directly visualized by time-resolved spectroscopy conformational substate transitions during catalytic turnover.

To address this limitation, we have labeled CaM with Alexa555 and Alexa647 fluorophores at defined locations to investigate CaM dynamics during enzyme turnover. CaM labeling was used because the nNOS flavohemoprotein contains 24 cysteine residues and 90 lysine residues, many of which are solvent exposed, preventing specific labeling of NOS with external fluorophores. Using Förster resonance energy transfer (FRET), we have studied the spatial and temporal dynamics of CaM bound to nNOS when nNOS is reduced with NADPH using rapid mixing stopped-flow spectrophotometry. We demonstrate also how use of a flavin analogue (5-deazaflavin-mononucleotide; 5-dFMN)[66,67] in place of FMN can simplify the correlation of structural transitions with NOS reaction chemistry. Our approach is general and mutatis mutandis could be adopted with other complex multicenter redox enzymes.

■ EXPERIMENTAL SECTION

The Supporting Information contains details of chemical suppliers and established methods for cloning, expression, and purification of CaM, nNOS, and the C-terminal kinase domain of FAD synthetase. Likewise, the Supporting Information documents contain methods for the enzymatic synthesis of 5-deazaflavin mononucleotide (5-dFMN) from 5-deazariboflavin along with conditions and instrumentation used for nNOS steady-state turnover assays, static fluorescence, and circular dichroism measurements.

Preparation of 5-dFMN Reconstituted NOS. The FMN cofactor was removed from NOS using immobilized metal affinity chromatography.[68] Briefly, 10 mg of purified NOS was applied to a 5 mL Ni-NTA column (GE Healthcare, Little Chalfont, U.K.) equilibrated with 40 mM HEPES buffer (pH 7.6) and supplemented with 10% glycerol and 150 mM NaCl at room temperature. The FMN was removed by washing the column with 25 mL of buffer supplemented with 2 M KBr at room temperature. Next, the column was transferred to a cold room (4 °C) and washed with 25 mL of cold buffer before elution of the apoprotein with buffer supplemented with 260 mM imidazole. For reconstitution with 5-dFMN, the eluted

apoprotein was added to a solution containing ∼0.5 mM 5-dFMN, 0.2 mM FAD, 0.2 mM tetrahydrobiopterin (H$_4$B), and 2 mM dithiothreitol (DTT) contained in 50 mM Tris-HCl (pH 8.0) buffer, supplemented with 10% glycerol and 150 mM NaCl, and incubated overnight at 4 °C with gentle mixing. The reconstituted protein was concentrated, and excess flavins and other cofactors were removed by applying the concentrated protein solution to an Econo-Pac DG10 column (Bio-Rad, Hempstead, U.K.) equilibrated in 40 mM HEPES buffer (pH 7.6) and supplemented with 10% glycerol and 150 mM NaCl. For anaerobic experiments, the final desalting step was performed in a Belle Technology anaerobic glovebox. Protein concentrations were determined at 444 nm in the presence of CO, using a molar extinction coefficient of 74 mM^{-1} cm^{-1} ($A_{444} - A_{500}$).

Conjugation of Extrinsic Fluorophores to T34C/T110C-CaM. A solid-state labeling methodology (SSL) was followed to achieve high-efficiency labeling of T34C/T110C-CaM with Alexa555 and Alexa647 maleimide.[69,70] T34C/T110C-CaM (5 μM) was incubated initially in 40 mM HEPES buffer (pH 7.1), supplemented with 5 mM dithiothreitol (DTT), 1 mM CaCl$_2$, 150 mM NaCl, and 10% glycerol for 2 h, at 4 °C. The protein was then recovered from solution by ammonium sulfate precipitation and pelleted by centrifugation. To remove traces of DTT, the T34C/T110C-CaM pellet was washed with 40 mM HEPES buffer (pH 7.1) supplemented with 5 M ammonium sulfate, 1 mM CaCl$_2$, 150 mM NaCl, and 10% glycerol and recovered by centrifugation. The protein pellet was then resuspended in 40 mM HEPES buffer (pH 7.6) supplemented with 1 mM CaCl$_2$ and 400 mM NaCl containing 100 μM of the desired fluorophore(s). Labeling reactions were incubated overnight, at 4 °C, in the dark. Excess fluorophore was separated from conjugated T34C/T110C-CaM by passing the sample down an Econo-Pace DG10 gel filtration column (Bio-Rad, Hempstead, U.K.) equilibrated with the desired buffer. For all anaerobic experiments this final step was performed in a nitrogen-purged glovebox using oxygen-free buffer. Each fluorophore (100 μM) was mixed with the protein to label T34C/T110C-CaM with an approximate 1:1 ratio of Alexa555 and Alexa647.

Stopped-Flow Spectrophotometry. All stopped-flow measurements were performed using an Applied Photophysics Ltd. (Leatherhead, U.K.) SC18MV instrument. The sample handling unit was placed inside a Belle Technology anaerobic glovebox (<5 ppm of O$_2$). All buffers and solutions were degassed by bubbling with oxygen-free nitrogen prior to entering the glovebox and left overnight to equilibrate to ensure removal of all traces of oxygen. All stopped-flow experiments were performed at 10 °C in 40 mM HEPES buffer (pH 7.6), supplemented with 10% glycerol and 150 mM NaCl.

For UV−vis measurements of nNOS flavin reduction, reactions were initiated by mixing 5 μM NOS with 100 μM NADPH (final concentrations) in the presence or absence of CaM and 1 mM Ca^{2+}. Under these conditions the observed rates are independent of the coenzyme concentration.[33] Multiple wavelength studies were carried out using a photodiode array (PDA) detector (Applied Photophysics Ltd., Leatherhead, U.K.). In single-wavelength studies, flavin reduction by NADPH was monitored at 485 nm, a heme isosbestic point.[71−73] For kinetic isotope effect (KIE) measurements single-wavelength studies of flavin reduction were performed using pro-R and pro-S NADP^{2}H. All measurements were repeated at least five times and are plotted as an average ±1 standard deviation.

Stopped-flow Förster resonance energy transfer (FRET) measurements were performed by mixing 0.25 μM nNOS/0.25 μM labeled T34C/T110C-CaM with 100 μM NADPH or 500 μM NADP$^+$ (final concentrations) in the presence of 0.5 mM Ca^{2+} and 5 μM H$_4$B. Dual-channel fluorescence was recorded with a 2 mm excitation path length using two photomultiplier tubes (PMT), including a R1104 red-sensitive photomultiplier detector (Applied Photophysics Ltd., Leatherhead, U.K.) to increase signal to noise for the acceptor channel. The donor channel was fitted with a 600 ± 5 nm bandwidth pass (ThorLabs, Ely, U.K.) filter, while the changes in fluorescence emission of the acceptor were monitored using a 650 nm cut-on filter (ThorLabs, Ely, U.K.). All measurements were repeated at least five times and are plotted as an average ±1 standard deviation. Data were analyzed and interpreted using methods previously described.[11,12] This analysis involved subtracting the percentage emission of the single-labeled CaM-bound fluorophore (Donor- or Acceptor-T34C/T110C-CaM) from the percentage emission of the corresponding fluorophore in the double-labeled CaM (DonorAcceptor-T34C/T110C-CaM) to extract the fluorescence changes associated with FRET alone.

nNOS tryptophan emission changes upon binding NADP$^+$ were monitored by mixing 0.2 μM nNOS/0.2 μM CaM (final concentration) with varying concentrations of NADP$^+$, in the presence of 0.5 mM Ca^{2+}. All emission changes associated with tryptophan were recorded using a stopped-flow cell with a 2 mm excitation path length. Tryptophan was excited at 295 nm, and emission changes were followed using a 340 nm cutoff filter.

All kinetic traces were fitted to standard exponential decay functions using Origin Pro (software).

■ RESULTS AND DISCUSSION

FRET Reporter of CaM Conformation Bound to nNOS. Our experimental model for detecting both CaM dynamics and nNOS-bound CaM conformational change during the catalytic cycle of nNOS is shown in Figure 2. Since wild-type CaM has no native cysteine residues, we introduced two solvent-exposed Cys residues (T34C/T110C-CaM) using site-directed mutagenesis, thereby allowing the addition of fluorophores at two specific locations in CaM. Labeling efficiency was >90%, and there was no recordable nonspecific fluorophore−CaM conjugation (data not shown). This double-cysteine-containing CaM protein has been used previously to monitor CaM dynamics in a variety of published fluorescence studies,[22,64,70,74,75] and it is useful here for probing intra CaM dynamics on binding to nNOS. This follows because (i) the position of the fluorophore binding sites, one on each of the N- and C-terminal calcium-binding globular domains of CaM, allows small changes in CaM conformation to be detected, (ii) the two maleimide labeling sites are located far away from the calcium-binding pockets on calmodulin and have little or no reported effect on the CaM−calcium interaction, and (iii) the effect of mutagenesis, as well as addition of the bulky fluorophore molecule to CaM, has no noticeable effect on the known catalytic ability of CaM to stimulate nNOS steady-state turnover (Figure S1 in the Supporting Information). On the basis of predicted fluctuations in distance between the two fluorophore labeling sites when CaM shifts between "open" and "closed" conformations (∼15−60 Å; Figure 2A), we selected
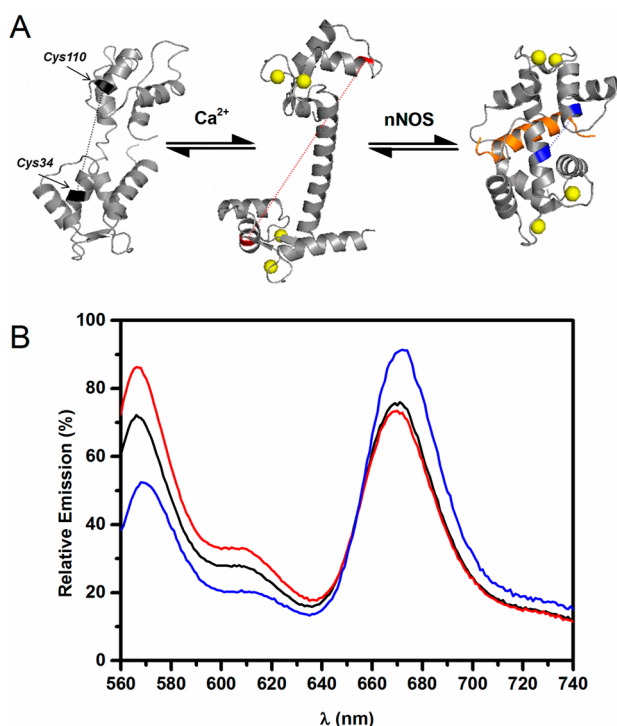
Figure 2. Ligand binding and the dynamic landscape of CaM. (A) Structures of apo (PDB_1CLL, shown on the left), Ca²⁺-bound (PDB_1CFC, shown in the middle) and both Ca²⁺/nNOS-peptide-bound forms of CaM (PDB_2O60, shown on the right). Divalent calcium ions are shown as yellow spheres, and the nNOS peptide is represented as an orange ribbon. The distances between the α-carbon atoms of the two fluorophore labeling sites (Cys34 and Cys110; highlighted in red) are 27, 52.4, and 12.4 Å for the apo, Ca²⁺-bound and the Ca²⁺/nNOS-bound forms, respectively. (B) Normalized fluorescence emission spectra showing ratiometric changes in the donor and acceptor emission. Samples: Alexa555-Alexa647 labeled T34C/T110C-CaM (black); T34C/T110C-CaM plus Ca²⁺ (red); T34C/T110C-CaM plus Ca²⁺ and nNOS (blue). All data in (B) were normalized to the emission maxima of their respective donor-only sample, and any emission changes observed from directly exciting the acceptor were corrected for by subtracting away from the double-labeled sample containing the same amount of acceptor (see Figures S3 and S4 in the Supporting Information). Conditions are described in the Experimental Section.

the fluorophore pair of Alexa555 (Donor, D) and Alexa647 (Acceptor, A) with a calculated Förster radius (R_0) of 47 Å. This allows the monitoring of subtle changes in CaM dynamics by Förster resonance energy transfer (FRET). Note, however, that not all labeled CaM molecules will undergo FRET due to the random nature of the labeling strategy. The selection of the fluorophore pair took into account also the fluorescence excitation spectra of both fluorophores (λ_{max} values of 555 and 645 nm for donor and acceptor fluorophores, respectively), which are red-shifted from the nNOS and CaM intrinsic fluorophores (flavins and aromatic amino acids). Thus, the analysis of FRET data (a reporter of CaM dynamics) is not compromised by undesirable fluorescence emission (Figure S2 in the Supporting Information).

Prior to conducting stopped-flow FRET studies to monitor the dynamics of nNOS-bound CaM, we recorded and analyzed fluorophore labeled-T34C/T110C-CaM fluorescence emission to see if our experimental model for tracking CaM dynamics fit to previously published ideas of how the conformational

landscape of CaM adjusts on ligand binding. Relevant CaM structures determined by X-ray crystallography[76] and NMR spectroscopy[77] are shown in Figure 2, along with the ratiometric changes in the equimolar donor to acceptor labeled (DA) T34C/T110C-CaM emission when CaM binds Ca²⁺ and nNOS (see Figures S3 and S4 in the Supporting Information for unprocessed data, including single fluorophore labeled D/A-T34C/T110C emission under the same conditions, and for information on data normalization). The altered fluorescence data indicate a change in the conformational landscape of apo-CaM on binding Ca²⁺. This shift in conformation from a "closed" to a more "open" form is evident from the reduced FRET efficiency: an increase in donor emission at 570 nm and a decrease in acceptor emission at 670 nm relative to fluorophore emission in the Ca²⁺-free DA-T34C/T110C-CaM when fluorophores were excited at 555 nm. When the fluorophore labeled apo-T34C/T110C-CaM was incubated with both Ca²⁺ and nNOS, an increase in the acceptor emission along with an anticorrelated response in donor emission were observed. This recorded FRET change is indicative of CaM forming a compact conformer with short Cys34-Cys110 distances, previously observed from published structural data of NOS[57] and nNOS peptides[78] bound to CaM.

Prior to performing time-resolved experiments, we assessed the possibility for inter-CaM FRET (FRET from CaM-CaM across the nNOS homodimer), which in principle could affect the interpretation of nNOS-bound intra-CaM FRET data (i.e., FRET within the individual nNOS-bound CaM proteins). Two separate batches of T34C/T110C-CaM were labeled with either donor or acceptor fluorophores, giving two separate and single-labeled CaM samples (D- and A-T34C/T110C-CaM). An equimolar mix of the D and A single-labeled T34C/T110C-CaM was added to 1 mol equiv of nNOS, and no FRET was observed across the nNOS dimer (Figure S5 in the Supporting Information). These data are in agreement with recently published cryo-EM structures[40] of native NOS proteins, which show the distances (>90 Å) between the two nNOS-bound CaM molecules to be outside the range for efficient energy transfer between the fluorophore pair.

Electron Transfer Kinetics in nNOS in the Presence and Absence of CaM. We probed the kinetics of NADPH-dependent nNOS flavin reduction by transient absorption stopped-flow spectrophotometry under pseudo-first-order conditions (20-fold excess NADPH).[33] nNOS is a complex enzyme with multiple cofactors (FAD, FMN, and heme) that are rich in optical features spanning the UV−visible spectrum. To study reduction of the nNOS flavins (FAD and FMN) by stopped-flow spectrophotometry, we followed the quenching of flavin absorbance at 485 nm, an isosbestic point for heme.[71−73] Stopped-flow traces reporting on nNOS (±CaM) flavin reduction, along with their respective exponential fits, are presented in Figure 3. Transients were fit optimally to five exponential terms (Figure 4B) over a time scale of 2 μs to 200 s. However, given that the nNOS-CaM steady-state turnover values, k_{cat}, for NO formation and NADPH consumption at 10 °C are ∼0.1 and 0.3 s⁻¹, respectively, we focus here only on the first four kinetic phases, as the slow fifth phase (with a rate constant of ∼0.01 s⁻¹) is not relevant to catalysis (Figure 3). Four resolvable kinetic phases have been seen previously in studies of the isolated nNOS reductase domain,[33,79] and in line with the study by Knight and co-workers,[33] we observed no appreciable increase in the rate of flavin reduction in full length nNOS in the presence of CaM in comparison with its absence.
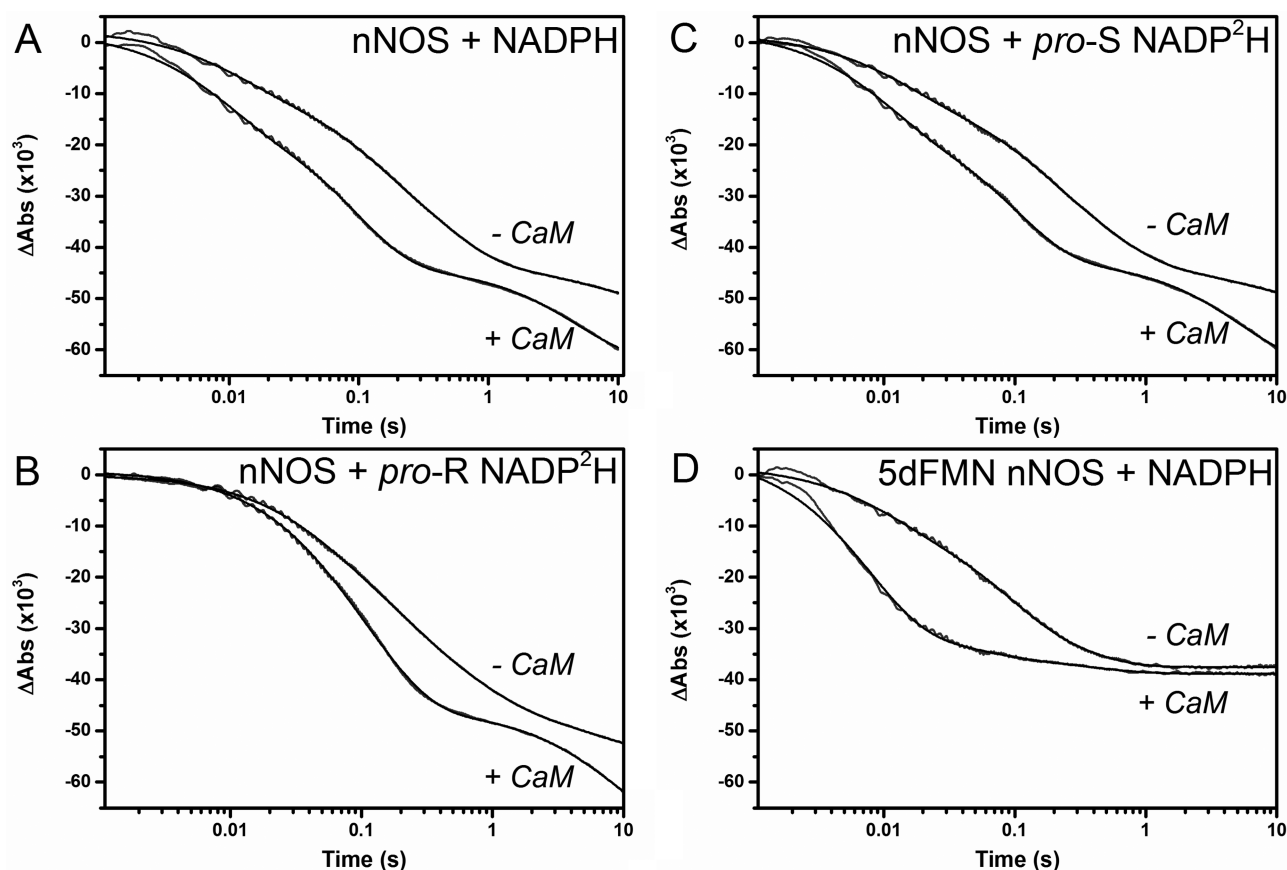
Figure 3. Anaerobic stopped-flow transients obtained at 485 nm on mixing 5 μM NOS (final concentration) with a 20-fold excess of NADPH in the presence or absence of CaM: (A) native NOS mixed with NADPH; (B) native NOS mixed with pro-S NADP^{2}H; (C) native NOS mixed with pro-R NADP^{2}H; (D) 5-dFMN-substituted NOS mixed with NADPH. Data and respective fits to an equation describing four sequential exponential processes are shown. Measurements were performed at least twice with different NOS preparations. Representative transients shown are the average of six to eight individual traces.

CaM does nonetheless have an effect on the relative amplitudes of the individual kinetic phases. These CaM-dependent influences on the amplitudes of kinetic phases are significant in all four phases (Figure 3 and Table 1), and as previous studies have implied,[34] it is likely that CaM has a role in governing nNOS flavin redox potentials. Alongside a CaM-induced structural change of nNOS that will affect the electron transfer geometry/distance, any alteration in redox potentials might also account for observed stimulation of electron transfer rates from nNOS FMN to the extrinsic partner protein cytochrome c in comparison to CaM-free nNOS (Table S1 in the Supporting Information).

The involvement of the four observed kinetic phases observed in stopped-flow studies of nNOS flavin reduction by NADPH in the enzyme catalytic cycle was probed by kinetic isotope effect (KIE) measurements using site specifically deuterated NADPH (pro-R and pro-S NADP^{2}H). KIE values were significant for the first three phases observed in stopped-flow studies of flavin reduction when excess pro-R (but not pro-S) NADP^{2}H is mixed with nNOS (Table S2 in the Supporting Information). The KIE values observed for the first three kinetics phases suggest that they report on hydride transfer from NADPH to FAD. These phases, however, do not map to discrete mechanistic steps, as the electron transfer steps are reversible and coupled. This accounts for the observation of primary KIEs in each of the first three phases measured in our stopped-flow studies. Below we demonstrate that interflavin

electron transfer is predominantly associated with the fourth kinetic phase in studies with nNOS that contains 5-dFMN rather than the conventional FMN (vide infra).

Direct Monitoring of CaM Dynamics during Catalytic Turnover of nNOS. We have used FRET stopped-flow spectroscopy to detect transient nNOS-bound CaM conformations that appear during the reaction cycle of nNOS. Donor/acceptor fluorophore-conjugated T34C/T110C-CaM (DA-T34C/T110C-CaM) was bound to nNOS in equimolar concentration and rapidly mixed with NADPH. The time-resolved fluorescence emission was followed on the same time scale as the nNOS reaction chemistry (vide supra). nNOS-bound DA-T34C/T110C-CaM was also mixed with buffer only in order to assess any potential photobleaching over the time scale of the rapid mixing experiments (200 s). No changes in emission were recorded over this time period for the acceptor fluorophore, and very small changes (~1%) were observed for the donor fluorescence. Since these emission changes were minor, they were omitted from subsequent analysis of all fluorescence emission data. FRET data representing the single-turnover conformational changes of nNOS-bound CaM on reduction with NADPH are shown in Figure 4A,B. Here the represented time-resolved donor and acceptor fluorescence emission changes are a deconvolution from other contributions to the emission response (Figure S7 in the Supporting Information), most notably the spectral changes in the nNOS bound chromophores (heme and flavins). We extracted the
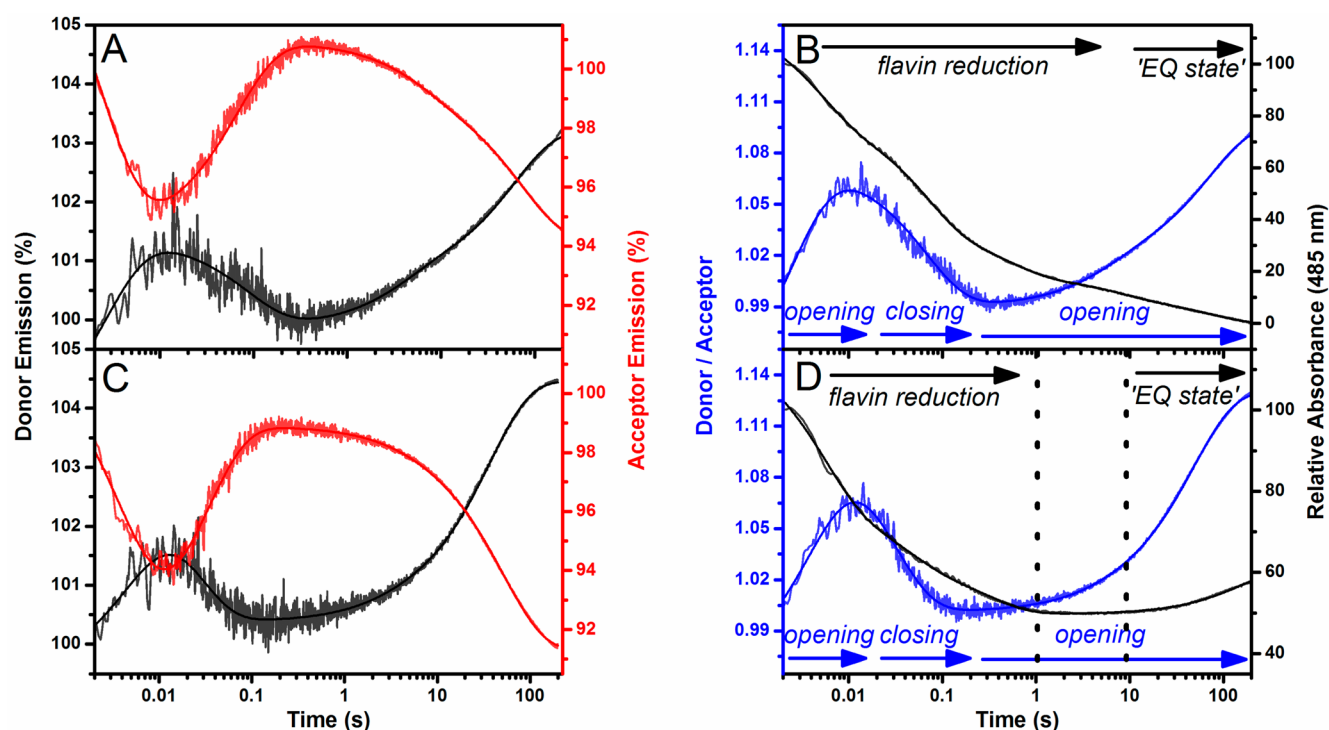
Figure 4. Dynamics of nNOS-bound CaM during NADPH-driven nNOS flavin reduction with native (panels A and B) and 5-dFMN (panels C and D) nNOS. (A) and (C) show the time-resolved anticorrelated emission changes of donor and acceptor fluorophore labeled T34C/T110C-CaM bound in equimolar concentrations to nNOS and 5-dFMN nNOS, respectively, on mixing with excess NADPH in a stopped-flow instrument. (B) and (D) show NADPH reduction of native and 5-dFMN nNOS recorded over 200 s (black) for the reaction between 5 μM nNOS bound to equimolar DA-T34C/T110C-CaM on mixing with excess NADPH along with the ratio of donor toacceptor fluorophores (blue) representing defined CaM "opening" (increased Cys−Cys distances) and "closing" (decreased Cys−Cys distances) steps during turnover. The first four rate constants associated with nNOS flavin reduction are relevant to enzyme turnover and have been labeled accordingly as "flavin reduction"; the slow phase is not relevant to steady-state turnover and has been termed the "EQ" state (see main text for a more detailed discussion). The area between the black dotted lines in (D) (~1−11 s) corresponds to the interflavin electron transfer step that is lost in the 5-dFMN nNOS variant. See the Experimental Section for details on conditions and instrumentation used.

Table 1. Kinetic Parameters Extracted from Figure 3[a]

NOS	reductant	k_1 (s^{-1})	ΔA_1	k_2 (s^{-1})	ΔA_2	k_3 (s^{-1})	ΔA_3	k_4 (s^{-1})	ΔA_4
native	NADPH	206.6 (67.1)	0.009 (0.003)	41.2 (27.3)	0.013 (0.003)	3.5 (1.4)	0.022 (0.008)	0.53 (0.28)	0.009 (0.005)
native	pro-S NADP^{2}H	197.6 (96.9)	0.008 (0.004)	38.3 (26.6)	0.013 (0.001)	2.5 (0.1)	0.026 (0.006)	0.29 (0.08)	0.009 (0.011)
native	pro-R NADP^{2}H	23.2 (0.6)	0.014 (0.004)	5.4 (0.1)	0.019 (0.001)	1.3 (0.1)	0.017 (0.001)	0.23 (0.07)	0.011 (0.001)
5-dFMN	NADPH	231.0 (13.4)	0.008 (0.004)	22.4 (4.2)	0.013 (0.007)	4.8 (0.7)	0.014 (0.001)	ND	ND
native + CaM	NADPH	216.4 (30.5)	0.022 (0.009)	20.9 (40.4)	0.023 (0.012)	4.1 (5.7)	0.010 (0.06)	0.10 (0.06)	0.025 (0.017)
native + CaM	pro-S NADP^{2}H	150.6 (5.3)	0.021 (0.002)	9.9 (1.6)	0.025 (0.003)	1.5 (0.4)	0.002 (0.001)	0.09 (0.06)	0.040 (0.026)
native + CaM	pro-R NADP^{2}H	50.9 (3.8)	0.010 (0.007)	8.8 (0.3)	0.045 (0.004)	0.68 (0.17)	0.006 (0.006)	0.06 (0.03)	0.028 (0.001)
5-dFMN + CaM	NADPH	228.2 (19.4)	0.024 (0.014)	53.0 (6.2)	0.011 (0.002)	5.5 (2.5)	0.005 (0.001)	ND	ND

[a]Observed rate constants (k) and absorbance changes (ΔA) determined by fitting transients in Figure 3 to exponential decay functions. Estimated errors are given in parentheses. ND = not detected.

Table 2. Rate Constants (k), Relative Fluorescence Changes (ΔC), and Ordinate Intercept (y0) Values Determined from Fitting Donor/Acceptor Fluorescence Transients (Figure 4B,D) to Exponential Decay Functions[a]

NOS	k_1 (s^{-1})	ΔC_1	k_2 (s^{-1})	ΔC_2	k_3 (s^{-1})	ΔC_3	k_4 (s^{-1})	ΔC_4	y0
native	274 (47)	−0.11 (0.01)	15.6 (2.1)	0.09 (0.01)	0.17 (0.05)	−0.03 (0.00)	0.014 (0.002)	−0.080 (0.002)	1.10 (0.02)
5-dFMN	205 (38)	−0.14 (0.02)	33.2 (5.2)	0.11 (0.01)	0.35 (0.36)	−0.01 (0.00)	0.021 (0.001)	−0.116 (0.003)	1.13 (0.02)

[a]Estimated errors are given in parentheses.

fluorescence emission change associated with donor−acceptor fluorophore FRET by subtracting the single-labeled (donor or acceptor) T34C/T110C-CaM bound nNOS sample relative emission from the relative emission of the corresponding fluorophore in the double-labeled (donor and acceptor) T34C/T110C-CaM bound nNOS sample (for more information see

refs 11 and 12). Changes in the donor and acceptor emission were anti-correlated, indicative of changes in FRET efficiency, and were fit to a four-exponential decay function (Figure 4A).

FRET data, which are presented as a ratio of donor to acceptor emission (Figure 4B), clearly exemplify an opening of the compact CaM protein, which is bound to nNOS initially in

the oxidized form when it is rapidly mixed with NADPH. This opening is kinetically coupled to early stages of the flavin reduction chemistry (k_1), involving the formation of a mixture of enzyme species (i.e., predominantly a distribution of FAD hydroquinone and oxidized FAD-NADPH charge transfer (CT) species; see ref 33 for a more detailed discussion of the reaction mechanism). Following the formation of this predominantly more open CaM substate, time-dependent emission changes in the donor and acceptor fluorescence show CaM to close, revealing a more compact conformer with shorter interfluorophore distances. This subsequent closing of the transiently opened nNOS-bound CaM conformer occurs in a single kinetic process with a rate constant of 15.6 s^{-1}, which is similar to the k_2 value observed for flavin reduction (Tables 1 and 2). This predominantly closed CaM conformer appears to be structurally similar to the form of CaM bound to oxidized nNOS (i.e., it has the same FRET emission properties). The third rate constant (k_3) for flavin reduction appears not to be associated with intra-CaM conformational change on binding to nNOS (at least within the detection limits of the instrumental setup used). The observed rate constants associated with the fourth (k_4) and fifth (k_5) kinetic phases of nNOS flavin reduction correlate closely with observed kinetic phases that report on intraCaM dynamics (i.e., a well-defined decrease in CaM-bound fluorophore FRET efficiency is observed).

There are no crystallographic data for full length nNOS; thus, the orientation that CaM adopts in the nNOS calmodulin binding site is not known. Structures only exist for the isolated reductase component,[55,56] the oxygenase domain,[52−54] and the FMN domain bound to CaM.[57] Consequently, how the structure of nNOS is affected by the change in CaM structure is not known. Current models invoke a complex landscape for the FAD, FMN, and oxygenase domains, and the mechanism of electron transfer is thought to involve conformational sampling of the FMN domain to facilitate electron transfer from the FAD domain to the heme oxygenase component. CaM is implicated, albeit in an ill-defined way, in this conformational sampling mechanism and is known to assist electron transfer from the FMN domain to the heme oxygenase. What we see for the first time from the current study is that CaM itself undergoes complex structural transitions during the catalytic cycle of nNOS, and these dynamic changes are likely central to the conformational sampling mechanism and the coordination of electron delivery from the FAD domain to the heme oxygenase.

Our FRET studies suggest that changes in the CaM conformation are coupled to early stages of flavin reduction, specifically FAD (but not FMN) reduction. To test this idea further, we have exploited the use of the FMN derivative 5-deazaflavin mononucleotide (5-dFMN),[66,67] which cannot stabilize the flavin semiquinone species. Incorporation of this analogue in nNOS is therefore expected to block FAD to FMN transfer in nNOS but still enable reduction of the FAD domain by NADPH. The availability of 5-dFMN nNOS would therefore simplify the redox chemistry in stopped-flow studies with NADPH and enable study of conformational change by FRET, while (importantly) retaining the overall structural integrity of nNOS.

New Form of nNOS Containing 5-Deazaflavin-Mono-nucleotide (5-dFMN). We simplified stopped-flow analysis of electron transfer in nNOS by preventing electron flow to the FMN and oxygenase domains, enabling more precise correlation of CaM conformational change with redox chemistry. This was achieved by substituting the natural FMN cofactor with the flavin biomimetic 5-dFMN. The affinity of the FMN cofactor for NOS is known to be less than that of the tightly bound FAD and heme cofactors.[45] The FMN cofactor was removed from nNOS using the weak chaotropic agent potassium bromide.[68] Apo-flavoproteins can generally be reconstituted with flavin derivatives modified at the isoalloxazine moiety, since the major interactions of the protein with the cofactor are associated with the N10 side chain.[68,80] 5-dFMN is structurally similar to conventional FMN and has been used previously as a biomimetic with other flavoproteins.[80] By incubating 5-dFMN with FMN-depleted nNOS the FMN binding site was replenished with 5-dFMN. Differences in the spectral properties of native and 5-dFMN bound nNOS (specifically, a decrease in absorbance at ∼450 and ∼380 nm and an increase in absorbance at ∼400 and ∼340 nm; Figure S11 in the Supporting Information) are entirely consistent with the known absorption properties of 5-dFMN and FMN (Figure S12 in the Supporting Information). Moreover, the secondary structure of 5-dFMN nNOS, determined by near-UV circular dichroism (CD), is essentially identical with that of native nNOS (Figure S10 in the Supporting Information). The overall protein secondary structure is therefore retained following replacement of FMN with 5-dFMN.

The activity of the reconstituted 5-dFMN nNOS enzyme was investigated using a variety of enzymatic steady-state turnover assays. In addition to reduction of the heme in the oxygenase domain, the diflavin reductase domain of nNOS is able to reduce artificial electron acceptors such as cytochrome c (cyt c) and ferricyanide. Cyt c accepts electrons only from the FMN cofactor of nNOS, but ferricyanide accepts electrons from both the FAD and FMN cofactors (Scheme S1 in the Supporting Information).[71] Using steady-state assays of cyt c and ferricyanide reduction, as well as monitoring NADPH depletion and NO formation, electron flow through the various NOS cofactors can be established. Exchange of the FMN cofactor for 5-dFMN completely abolished steady-state cytochrome c reduction and NO formation and almost completely eliminated NADPH consumption (∼1% activity remained in comparison with native nNOS, which is attributed to reoxidation of nNOS-bound FADH$_2$ by molecular oxygen).[81] Ferricyanide reduction is maintained in 5-dFMN nNOS (Table S1 in the Supporting Information), consistent with the known ability of the FAD domain to transfer electrons to ferricyanide. That activities known to be dependent on interflavin electron transfer are abolished is consistent with our expectation that interflavin electron transfer is blocked in 5-dFMN nNOS as a result of the very unfavorable reduction potential for 5-dFMN semiquinone formation.[66] This was further corroborated by anaerobic reductive titration of native nNOS and 5-dFMN NOS with both NADPH (electrons enter only via the FAD domain) and dithionite (DT), where electrons can access each of the flavin/heme cofactors directly. With NADPH (Figure S11 in the Supporting Information), the absorbance changes are consistent with loss of oxidized flavin and appearance of the blue flavin semiquinone species, which, as reported previously, is a consequence of interflavin electron transfer following initial reduction of FAD to FADH$_2$ by NADPH.[33,82] With 5-dFMN nNOS (reduced by NADPH), depletion of oxidized flavin is observed, but there is minimal appearance of the blue semiquinone signature. This is consistent with the expected block on electron transfer to the FMN domain. In contrast, reductive titration with DT (Figure S11) results in full
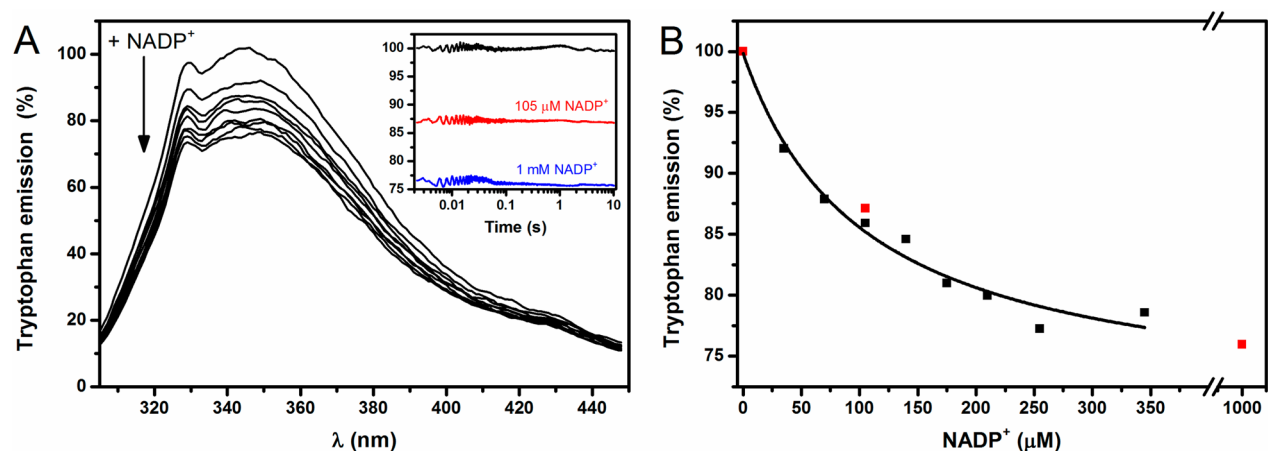
Figure 5. NADP + nNOS binding occurring in the dead time of the stopped-flow instrument. (A) Fluorescence emission changes of the nNOS tryptophans in the nNOS:CaM complex upon binding the oxidized coenzyme $NADP^+$. The insert in (A) shows the tryptophan emission changes associated with $NADP^+$ binding to the nNOS:CaM complex recorded in the dead time of the stopped-flow instrument. In the inset the black trace represents the mixing of the nNOS:CaM complex with buffer alone, while red and blue are labeled accordingly with the final $NADP^+$ concentrations used in the stopped-flow study. (B) Static titration data (black) and the emission changes recorded in the dead time of the stopped-flow instrument (red) for the $NADP^+$-dependent changes in the tryptophan emission of the nNOS:CaM complex. Data in (B) were fitted to a hyperbolic binding function, which gives an apparent K_d value for the nNOS:CaM−$NADP^+$ complex of 106 ± 27 μM.

reduction (flavins and heme) of nNOS and 5-dFMN nNOS. These findings are consistent with a variety of previously published papers that emphasize the different redox chemistry of flavin and 5-deazaflavin[66,67] in relation to semiquinone stabilization, which is an obligate intermediate in the catalytic cycle of NOS.[33]

Internal Electron Transfer Is Prevented in 5-dFMN nNOS. Similar to the transient absorption stopped-flow studies of native nNOS, we measured the single-turnover NADPH-dependent reduction of 5-dFMN nNOS by rapid mixing of oxidized 5-dFMN nNOS with excess NADPH (20 mol equiv).[33] Stopped-flow transients measured over 10 s are shown in Figure 3. The blue shift in 5-dFMN spectral features allows monitoring of the nNOS-bound FAD cofactor alone at 485 nm (and see accompanying spectra recorded with a photodiode array in Figure S6 in the Supporting Information). In contrast to comparable experiments performed with nNOS (vide supra), where flavin reduction was described by four kinetic phases over 10 s, in the case of 5-dFMN nNOS flavin reduction (monitored at 485 nm) flavin reduction occurred in three kinetic phases. Observed rate constants determined by fitting to a triple-exponential equation and associated amplitude changes are similar to those recorded for the native enzyme (k_1 to k_3). The slower fourth phase seen for nNOS is absent in studies with 5-dFMN NOS, consistent with the inability to transfer electrons from FAD to 5-dFMN.

The slow fourth phase observed with nNOS has an observed rate constant similar to that of k_{cat} in steady-state NO production and NADPH depletion assays (Table S1 in the Supporting Information). This suggests that this kinetic phase contributes to rate limitation in steady-state turnover, together with other established steps in the catalytic cycle (notably FMN to heme electron transfer).[18] We emphasize again that this is a kinetic phase associated with an observed spectral change and does not report on a single mechanistic step. As with other diflavin reductases such as the well-characterized cytochrome P450 reductase,[82] the kinetic phases observed for nNOS report on the formation of a distribution of enzyme intermediates. In all likelihood, the slow fourth phase reports not only on

interflavin electron transfer but also on FMN to heme electron transfer in a single kinetic process (but heme reduction is not observed at the wavelength we monitored). The finding that interflavin electron transfer is relatively slow in nNOS is in line with a previous study on the isolated nNOS reductase domain. This study suggested that interflavin electron transfer might also be gated by $NADP^+$ release,[33] consistent with steady-state and isotope effect studies reported by others.[83]

Over extended time scales (200 s) stopped-flow studies with 5-dFMN NOS also revealed an additional (fourth) kinetic phase (Figure 4D). This step has the same kinetics as formation of the native nNOS "EQ state" (~ 0.01 s^{-1} for native and 5-dFMN nNOS), albeit with a different associated amplitude (0.006 and −0.006 for native and 5-dFMN nNOS). This "EQ state" has been discussed in many studies with diflavin oxidoreductases as a signal that likely results from further conformational change and/or further oxidation of NADPH attributed to thermodynamic relaxation through disproportionation reactions.[33,82] The formal attribution of this phase to mechanistic processes is complicated. It is not relevant to steady-state catalysis and for that reason we have chosen not to comment on it further in this work.

Correlating Conformational Change with Early Steps in Electron Transfer in 5-dFMN nNOS. With the availability of 5-dFMN NOS we were able to investigate conformational changes linked to FAD reduction, in the absence of electron transfer to the FMN and oxygenase domains. Stopped-flow FRET data for the reaction between 5-dFMN nNOS-bound to donor−acceptor labeled CaM and NADPH are shown in Figures 4C,D. Anti-correlated donor and acceptor emission transients along with FRET data (i.e., the ratio of donor and acceptor emission) were optimally fit to four exponential decays over 200 s. Rate constants associated with the four phases are similar to those recorded for donor−acceptor labeled CaM bound to native nNOS (Table 2). In addition, the directionality of conformational change (i.e., "opening" and "closing" of CaM) for 5-dFMN nNOS-bound CaM mimics that for nNOS. Some differences in FRET amplitudes (degree of "opening" or "closing") between nNOS and 5-dFMN nNOS-
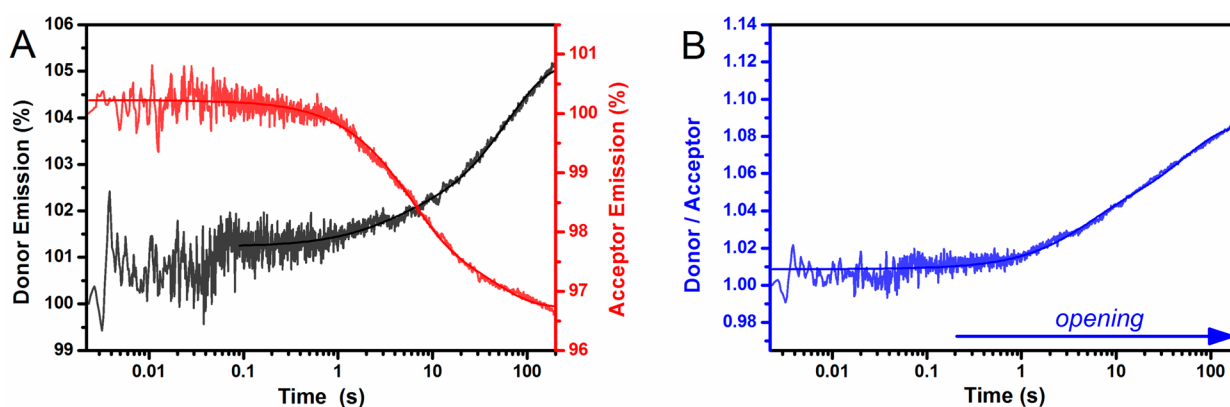
Figure 6. NADP$^+$ binding to nNOS driving conformational change of CaM in the nNOS−CaM complex. (A) Time-resolved anticorrelated emission changes of donor and acceptor fluorophore labeled T34C/T110C-CaM bound in equimolar concentrations to nNOS when mixed with excess NADP$^+$ (500 μM final concentration) in a stopped-flow instrument. (B) Ratio of donor to acceptor fluorophores presented in (A) representing the "opening" of nNOS-bound CaM (i.e., an increase in the Cys−Cys distance). See the Experimental Section for details on conditions used and instrument setup.

bound CaM can be seen in the third and fourth phases. In nNOS enzyme these phases are associated with the kinetics of interflavin electron transfer and formation of the "EQ state", respectively.

The data indicate that interflavin electron transfer/FMN reduction do not drive CaM conformational change, as this step is blocked in 5-dFMN nNOS. We infer therefore that the observed FRET conformational changes are associated with early steps in the electron transfer sequence, which relate either to NADPH binding and/or reduction of the FAD. We note that the extended C-terminal tail of nNOS (and other NOS isoforms) needs to be displaced from the NADPH binding site on mixing nNOS with NADPH[61,71,79,84,85] and this might be a mechanism for connecting binding and/or electron transfer events with the observed FRET signals that report on intra-CaM motions.

NADP$^+$ Binding Remodels the IntraCaM landscape in nNOS but over Longer Time Scales. We also investigated the effects of coenzyme binding in the absence of nNOS reduction on the modulation of the intra-CaM conformational landscape. In this case, NADP$^+$ was used rather than NADPH to prevent reduction of nNOS flavins. Quenching of intrinsic nNOS tryptophan fluorescence emission was used to monitor the binding of NADP$^+$. By titrating nNOS (bound to DA-T34C/T110C-CaM) with NADP$^+$, we were able to measure a dissociation constant, K_d, of 106 ± 27 μM for the enzyme−coenzyme complex. By following Trp fluorescence in the stopped-flow instrument when rapidly mixing saturating concentrations of NADP$^+$ with the nNOS DA-T34C/T110C-CaM complex, the observed rate of coenzyme binding was obtained. The expected fluorescence changes associated with coenzyme−enzyme interaction occurred within the dead time (1.5 ms) of the stopped-flow instrument (Figure 5). Consequently, and in line with other diflavin oxidoreductases,[12] we conclude that NADP$^+$ binding to nNOS is rapid (>500 s^{-1} at 10 °C).

To study the effects of NADP$^+$ binding on nNOS-bound intra-CaM dynamics, donor−acceptor fluorophore labeled-T34C/T110C-CaM bound to 1 molar equiv of nNOS was mixed with saturating concentrations of NADP$^+$. FRET stopped-flow transients representing the nNOS-bound intra-CaM dynamics for the reaction between NADP$^+$ and equimolar concentrations of nNOS and T34C/T110C-CaM are shown in

Figure 6. No FRET changes were observed in the dead time of the stopped-flow instrument, indicating that there are no binding induced nNOS-bound CaM conformational changes. However, conformational change was observed only over extended time scales (up to 200 s) and transients reporting on nNOS-bound CaM conformational change were analyzed using a double-exponential function (Figure 6). The two observed kinetic phases have rate constants similar in value to k_3 and k_4 recorded for CaM dynamics in NADPH-reduced native and 5-dFMN nNOS (Table 2 and Table S4 in the Supporting Information). The response to NADP$^+$ binding is therefore different from that observed in stopped-flow studies with NADPH, where CaM dynamics were observed on shorter time scales and were associated with NADPH binding and FAD reduction. This suggests either (i) that the mode of interaction of NADP$^+$ and NADPH with nNOS is sufficiently different so as to elicit different responses in the remodelling of the CaM landscape or (ii) that redox changes in the FAD are also required to drive the relatively fast remodeling of the CaM landscape in stopped-flow studies of nNOS reduction with NADPH. Either way, it is clear that NADPH binding/FAD reduction is the primary trigger for the remodeling CaM rather than internal electron transfer to FMN/heme.

■ CONCLUDING REMARKS

It has been known for some time that ligand−protein interactions affect the conformational landscape of enzyme molecules.[14,86] Ligand-induced conformational changes have been documented previously in the diflavin oxidoreductase family and by NADP$^+$ binding in nNOS.[20] Moreover, crystallographic studies of NOS and other diflavin oxidoreductases have also implicated a role for ligand-induced conformational change in these enzymes, particularly in relation to conformational sampling of the FMN binding domain in relation to the FAD and oxygenase domains (i.e., the so-called "input" and "output" states of nNOS).

A major and largely unmet challenge has been the need to correlate protein motions (i.e., in real time) across the catalytic cycle so that a more holistic understanding of the role of dynamics in enzyme mechanisms can be inferred. In this paper we have begun to address this limitation by correlating the dynamics of CaM bound to the reaction chemistry of nNOS during what is a highly complex reaction cycle. This has

enabled us to pinpoint major conformational changes in CaM as a function of time to correlate these changes with specific chemical steps in the reaction cycle and identify/suggest the mechanistic triggers for these major conformational adjustments. This extends appreciably our current understanding of nNOS dynamics inferred from structural, single-molecule, EPR, electron microscopy, and kinetic approaches, and it paves the way for similar analyses on other complex redox systems where knowledge of dynamics in relation to chemistry is important in advancing the mechanistic description of catalysis.

Our analysis has shown that major remodeling of the CaM landscape occurs during early phases of electron transfer during the NADPH-dependent reduction of nNOS. A combination of isotope effects, FRET studies, and use of 5-dFMN to block internal electron transfer has enabled more precise mapping of kinetic phases observed in stopped-flow experiments to domain-specific redox changes. Although these phases cannot be attributed to a single mechanistic step, we have demonstrated that binding and/or redox changes associated with the FAD domain are correlated with major remodeling of the bound CaM in nNOS. This remodeling is likely triggered in part through displacement of the C-terminal tail from the NADPH binding site by the incoming nicotinamide coenzyme, but other factors might also be in play. The approaches we have developed should find wider application in related studies with NOS isoforms, where simplification of the reaction chemistry and strategic positioning of fluorescence reporters can be used to inform not only on the dynamics of CaM but also on the relative orientations and time-dependent conformational remodeling of other domains in NOS enzymes.

■ ASSOCIATED CONTENT

Ⓢ Supporting Information

The Supporting Information is available free of charge on the ACS Publications website at DOI: 10.1021/acscatal.6b01280.

> Experimental details including cloning, expression, and purification of enzymes, biosynthesis of 5-dFMN from 5-dRF, circular dichroism, static fluorescence, and stopped-flow measurements (PDF)

■ AUTHOR INFORMATION

Corresponding Author

*N.S.S.: e-mail, nigel.scrutton@manchester.ac.uk; tel, +44 161 306 5152.

Author Contributions

T.M.H. and N.S.S. wrote the manuscript. N.G.H.L. developed and established the protocol for exchanging FMN for 5-dFMN in nNOS. T.M.H. developed and conducted all experiments apart from UV–vis stopped-flow assays, which were conducted by both N.G.H.L. and T.M.H. All authors contributed to data analysis and interpretation and have given approval to the final version of the manuscript.

Notes

The authors declare no competing financial interest.

■ ACKNOWLEDGMENTS

■ ABBREVIATIONS

nNOS, neuronal nitric oxide synthase; NOS, nitric oxide synthase; CaM, calmodulin; cyt *c*, cytochrome *c*; FRET, Förster resonance energy transfer; FAD, flavin adenine dinucleotide; FMN, flavin mononucleotide; 5-dRF, 5-deaza riboflavin; 5-dFMN, 5-deaza flavin mononucleotide

■ REFERENCES

(1) Rothlisberger, D.; Khersonsky, O.; Wollacott, A. M.; Jiang, L.; DeChancie, J.; Betker, J.; Gallaher, J. L.; Althoff, E. A.; Zanghellini, A.; Dym, O.; Albeck, S.; Houk, K. N.; Tawfik, D. S.; Baker, D. *Nature* **2008**, *453*, 190−195.

(2) Kaplan, J.; DeGrado, W. F. *Proc. Natl. Acad. Sci. U. S. A.* **2004**, *101*, 11566−11570.

(3) Anderson, A. C. *Chem. Biol.* **2003**, *10*, 787−797.

(4) Wilson, C.; Agafonov, R. V.; Hoemberger, M.; Kutter, S.; Zorba, A.; Halpin, J.; Buosi, V.; Otten, R.; Waterman, D.; Theobald, D. L.; Kern, D. *Science* **2015**, *347*, 882−886.

(5) Hay, S.; Scrutton, N. S. *Nat. Chem.* **2012**, *4*, 161−168.

(6) Nagel, Z. D.; Klinman, J. P. *Nat. Chem. Biol.* **2009**, *5*, 543−550.

(7) Villali, J.; Kern, D. *Curr. Opin. Chem. Biol.* **2010**, *14*, 636−643.

(8) Schwartz, S. D.; Schramm, V. L. *Nat. Chem. Biol.* **2009**, *5*, 551−558.

(9) Benkovic, S. J.; Hammes, G. G.; Hammes-Schiffer, S. *Biochemistry* **2008**, *47*, 3317−3321.

(10) Leferink, N. G. H.; Pudney, C. R.; Brenner, S.; Heyes, D. J.; Eady, R. R.; Hasnain, S. S.; Hay, S.; Rigby, S. E. J.; Scrutton, N. S. *FEBS Lett.* **2012**, *586*, 578−584.

(11) Hedison, T. M.; Hay, S.; Scrutton, N. S. *FEBS J.* **2015**, *282*, 4357−4375.

(12) Pudney, C. R.; Khara, B.; Johannissen, L. O.; Scrutton, N. S. *PLoS Biol.* **2011**, *9*, e1001222.

(13) Agafonov, R. V.; Wilson, C.; Otten, R.; Buosi, V.; Kern, D. *Nat. Struct. Mol. Biol.* **2014**, *21*, 848−853.

(14) Boehr, D. D.; Nussinov, R.; Wright, P. E. *Nat. Chem. Biol.* **2009**, *5*, 789−796.

(15) Mittermaier, A.; Kay, L. E. *Science* **2006**, *312*, 224−228.

(16) Henzler-Wildman, K. A.; Thai, V.; Lei, M.; Ott, M.; Wolf-Watz, M.; Fenn, T.; Pozharski, E.; Wilson, M. A.; Petsko, G. A.; Karplus, M.; Huebner, C. G.; Kern, D. *Nature* **2007**, *450*, 838−844.

(17) Myong, S.; Stevens, B. C.; Ha, T. *Structure* **2006**, *14*, 633−643.

(18) Leferink, N. G. H.; Hay, S.; Rigby, S. E. J.; Scrutton, N. S. *FEBS J.* **2015**, *282*, 3016−3029.

(19) Hay, S.; Brenner, S.; Khara, B.; Quinn, A. M.; Rigby, S. E.; Scrutton, N. S. *J. Am. Chem. Soc.* **2010**, *132*, 9738−9745.

(20) Sobolewska-Stawiarz, A.; Leferink, N. G. H.; Fisher, K.; Heyes, D. J.; Hay, S.; Rigby, S. E. J.; Scrutton, N. S. *J. Biol. Chem.* **2014**, *289*, 11725−11738.

(21) Pudney, C. R.; Hay, S.; Levy, C.; Pang, J.; Sutcliffe, M. J.; Leys, D.; Scrutton, N. S. *J. Am. Chem. Soc.* **2009**, *131*, 17072−17073.

(22) Johnson, C. K. *Biochemistry* **2006**, *45*, 14233−14246.

(23) Hoeflich, K. P.; Ikura, M. *Cell* **2002**, *108*, 739−742.

(24) Andersson, T.; Drakenberg, T.; Forsen, S.; Thulin, E. *Eur. J. Biochem.* **1982**, *126*, 501−505.

(25) Bayley, P.; Ahlstrom, P.; Martin, S. R.; Forsen, S. *Biochem. Biophys. Res. Commun.* **1984**, *120*, 185−191.

(26) Tjandra, N.; Kuboniwa, H.; Ren, H.; Bax, A. *Eur. J. Biochem.* **1995**, *230*, 1014−1024.

(27) Zhang, M.; Tanaka, T.; Ikura, M. *Nat. Struct. Biol.* **1995**, *2*, 758−767.

(28) Babu, Y. S.; Sack, J. S.; Greenhough, T. J.; Bugg, C. E.; Means, A. R.; Cook, W. J. *Nature* **1985**, *315*, 37−40.

(29) Wilson, M. A.; Brunger, A. T. *J. Mol. Biol.* **2000**, *301*, 1237−1256.

(30) Kahl, C. R.; Means, A. R. *Endocr. Rev.* **2003**, *24*, 719−736.

(31) Alderton, W. K.; Cooper, C. E.; Knowles, R. G. *Biochem. J.* **2001**, *357*, 593−615.

(32) Abusoud, H. M.; Yoho, L. L.; Stuehr, D. J. *J. Biol. Chem.* **1994**, *269*, 32047−32050.

(33) Knight, K.; Scrutton, N. S. *Biochem. J.* **2002**, *367*, 19−30.

(34) Dunford, A. J.; Rigby, S. E.; Hay, S.; Munro, A. W.; Scrutton, N. S. *Biochemistry* **2007**, *46*, 5018−5029.

(35) Feng, C.; Tollin, G.; Hazzard, J. T.; Nahm, N. J.; Guillemette, J. G.; Salerno, J. C.; Ghosh, D. K. *J. Am. Chem. Soc.* **2007**, *129*, 5621−5629.

(36) Feng, C.; Roman, L. J.; Hazzard, J. T.; Ghosh, D. K.; Tollin, G.; Masters, B. S. *FEBS Lett.* **2008**, *582*, 2768−2772.

(37) Smith, B. C.; Underbakke, E. S.; Kulp, D. W.; Schief, W. R.; Marletta, M. A. *Proc. Natl. Acad. Sci. U. S. A.* **2013**, *110*, E3577−E3586.

(38) Beaumont, E.; Lambry, J.; Gautier, C.; Robin, A.; Gmouh, S.; Berka, V.; Tsai, A.; Blanchard-Desce, M.; Slama-Schwok, A. *J. Am. Chem. Soc.* **2007**, *129*, 2178−2186.

(39) Yokom, A. L.; Morishima, Y.; Lau, M.; Su, M.; Glukhova, A.; Osawa, Y.; Southworth, D. R. *J. Biol. Chem.* **2014**, *289*, 16855−16865.

(40) Campbell, M. G.; Smith, B. C.; Potter, C. S.; Carragher, B.; Marletta, M. A. *Proc. Natl. Acad. Sci. U. S. A.* **2014**, *111*, E3614−E3623.

(41) Volkmann, N.; Martasek, P.; Roman, L. J.; Xu, X.; Page, C.; Swift, M.; Hanein, D.; Masters, B. S. *J. Struct. Biol.* **2014**, *188*, 46−54.

(42) Astashkin, A. V.; Chen, L.; Zhou, X.; Li, H.; Poulos, T. L.; Liu, K. J.; Guillemette, J. G.; Feng, C. *J. Phys. Chem. A* **2014**, *118*, 6864−6872.

(43) Astashkin, A. V.; Elmore, B. O.; Fan, W.; Guillemette, J. G.; Feng, C. *J. Am. Chem. Soc.* **2010**, *132*, 12059−12067.

(44) Ghosh, D. K.; Ray, K.; Rogers, A. J.; Nahm, N. J.; Salerno, J. C. *FEBS J.* **2012**, *279*, 1306−1317.

(45) He, Y.; Haque, M. M.; Stuehr, D. J.; Lu, H. P. *Proc. Natl. Acad. Sci. U. S. A.* **2015**, *112*, 11835−11840.

(46) Abusoud, H. M.; Stuehr, D. J. *Proc. Natl. Acad. Sci. U. S. A.* **1993**, *90*, 10769−10772.

(47) Panda, K.; Ghosh, S.; Stuehr, D. J. *J. Biol. Chem.* **2001**, *276*, 23349−23356.

(48) Siddhanta, U.; Presta, A.; Fan, B.; Wolan, D.; Rousseau, D. L.; Stuehr, D. J. *J. Biol. Chem.* **1998**, *273*, 18950−18958.

(49) Sagami, I.; Daff, S.; Shimizu, T. *J. Biol. Chem.* **2001**, *276*, 30036−30042.

(50) Stuehr, D. J.; Tejero, J.; Haque, M. M. *FEBS J.* **2009**, *276*, 3959−3974.

(51) Wei, C. C.; Crane, B. R.; Stuehr, D. J. *Chem. Rev.* **2003**, *103*, 2365−2383.

(52) Crane, B. R.; Arvai, A. S.; Ghosh, D. K.; Wu, C.; Getzoff, E. D.; Stuehr, D. J.; Tainer, J. A. *Science* **1998**, *279*, 2121−2126.

(53) Li, H.; Shimizu, H.; Flinspach, M.; Jamal, J.; Yang, W.; Xian, M.; Cai, T.; Wen, E. Z.; Jia, Q.; Wang, P. G.; Poulos, T. L. *Biochemistry* **2002**, *41*, 13868−13875.

(54) Raman, C. S.; Li, H.; Martasek, P.; Kral, V.; Masters, B. S.; Poulos, T. L. *Cell* **1998**, *95*, 939−950.

(55) Garcin, E. D.; Bruns, C. M.; Lloyd, S. J.; Hosfield, D. J.; Tiso, M.; Gachhui, R.; Stuehr, D. J.; Tainer, J. A.; Getzoff, E. D. *J. Biol. Chem.* **2004**, *279*, 37918−37927.

(56) Zhang, J.; Martasek, P.; Paschke, R.; Shea, T.; Masters, B. S.; Kim, J. J. P. *J. Biol. Chem.* **2001**, *276*, 37506−37513.

(57) Xia, C.; Misra, I.; Iyanagi, T.; Kim, J. J. *J. Biol. Chem.* **2009**, *284*, 30708−30717.

(58) Wang, M.; Roberts, D. L.; Paschke, R.; Shea, T. M.; Masters, B. S. S.; Kim, J. J. P. *Proc. Natl. Acad. Sci. U. S. A.* **1997**, *94*, 8411−8416.

(59) Piazza, M.; Futrega, K.; Spratt, D. E.; Dieckmann, T.; Guillemette, J. G. *Biochemistry* **2012**, *51*, 3651−3661.

(60) Brenner, S.; Hay, S.; Munro, A. W.; Scrutton, N. S. *FEBS J.* **2008**, *275*, 4540−4557.

(61) Craig, D. H.; Chapman, S. K.; Daff, S. *J. Biol. Chem.* **2002**, *277*, 33987−33994.

(62) Salerno, J. C.; Ray, K.; Poulos, T.; Li, H.; Ghosh, D. K. *FEBS Lett.* **2013**, *587*, 44−47.

(63) Brunner, K.; Tortschanoff, A.; Hemmens, B.; Andrew, P. J.; Mayer, B.; Kungl, A. J. *Biochemistry* **1998**, *37*, 17545−17553.

(64) Spratt, D. E.; Taiakina, V.; Palmer, M.; Guillemette, J. G. *Biochemistry* **2007**, *46*, 8288−8300.

(65) Persechini, A.; Quang-Kim, T.; Black, D. J.; Gogol, E. P. *FEBS Lett.* **2013**, *587*, 297−301.

(66) Hemmerich, P.; Massey, V.; Fenner, H. *FEBS Lett.* **1977**, *84*, 5−21.

(67) Blankenhorn, G. *Eur. J. Biochem.* **1976**, *67*, 67−80.

(68) Hefti, M. H.; Milder, F. J.; Boeren, S.; Vervoort, J.; van Berkel, W. J. H. *Biochim. Biophys. Acta, Gen. Subj.* **2003**, *1619*, 139−143.

(69) Kim, Y.; Ho, S. O.; Gassman, N. R.; Korlann, Y.; Landorf, E. V.; Collart, F. R.; Weiss, S. *Bioconjugate Chem.* **2008**, *19*, 786−791.

(70) Allen, M. W.; Urbauer, R. J.; Zaidi, A.; Williams, T. D.; Urbauer, J. L.; Johnson, C. K. *Anal. Biochem.* **2004**, *325*, 273−284.

(71) Roman, L. J.; Martasek, P.; Miller, R. T.; Harris, D. E.; de la Garza, M. A.; Shea, T. M.; Kim, J. J. P.; Masters, B. S. S. *J. Biol. Chem.* **2000**, *275*, 29225−29232.

(72) Haque, M. M.; Panda, K.; Tejero, J.; Aulak, K. S.; Fadlalla, M. A.; Mustovich, A. T.; Stuehr, D. J. *Proc. Natl. Acad. Sci. U. S. A.* **2007**, *104*, 9254−9259.

(73) Miller, R. T.; Martasek, P.; Omura, T.; Masters, B. S. S. *Biochem. Biophys. Res. Commun.* **1999**, *265*, 184−188.

(74) Drum, C. L.; Yan, S. Z.; Sarac, R.; Mabuchi, Y.; Beckingham, K.; Bohm, A.; Grabarek, Z.; Tang, W. J. *J. Biol. Chem.* **2000**, *275*, 36334−36340.

(75) Torok, K.; Tzortzopoulos, A.; Grabarek, Z.; Best, S. L.; Thorogate, R. *Biochemistry* **2001**, *40*, 14878−14890.

(76) Chattopadhyaya, R.; Meador, W. E.; Means, A. R.; Quiocho, F. A. *J. Mol. Biol.* **1992**, *228*, 1177−1192.

(77) Kuboniwa, H.; Tjandra, N.; Grzesiek, S.; Ren, H.; Klee, C. B.; Bax, A. *Nat. Struct. Biol.* **1995**, *2*, 768−776.

(78) Wu, G.; Berta, V.; Tsai, A. *J. Inorg. Biochem.* **2011**, *105*, 1226−1237.

(79) Konas, D. W.; Zhu, K.; Sharma, M.; Aulak, K. S.; Brudvig, G. W.; Stuehr, D. J. *J. Biol. Chem.* **2004**, *279*, 35412−35425.

(80) Manstein, D. J.; Massey, V.; Ghisla, S.; Pai, E. F. *Biochemistry* **1988**, *27*, 2300−2305.

(81) Xia, Y. *Antioxid. Redox Signaling* **2007**, *9*, 1773−1778.

(82) Gutierrez, A.; Lian, L. Y.; Wolf, C. R.; Scrutton, N. S.; Roberts, G. C. K. *Biochemistry* **2001**, *40*, 1964−1975.

(83) Wolthers, K. R.; Schimerlik, M. I. *Biochemistry* **2002**, *41*, 196−204.

(84) Tiso, M.; Tejero, J.; Panda, K.; Aulak, K. S.; Stuehr, D. J. *Biochemistry* **2007**, *46*, 14418−14428.

(85) Tiso, M.; Konas, D. W.; Panda, K.; Garcin, E. D.; Sharma, M.; Getzoff, E. D.; Stuehr, D. J. *J. Biol. Chem.* **2005**, *280*, 39208−39219.

(86) Koshland, D. E. *Proc. Natl. Acad. Sci. U. S. A.* **1958**, *44*, 98−104.